THREE-NUCLEON FORCE EFFECTS IN THE ANALYZING POWERS OF THE $\vec{d}p$ BREAKUP AT 130 MeV* **

A. Biegun[a], E. Stephan[a], St. Kistryn[b], K. Bodek[b], I. Ciepał[b]
A. Deltuva[c], E. Epelbaum[d], W. Glöckle[e], J. Golak[b]
N. Kalantar-Nayestanaki[f], H. Kamada[g], M. Kiš[f], B. Kłos[a]
A. Kozela[h], J. Kuroś-Żołnierczuk[b], M. Mahjour-Shafiei[f]
U.-G. Meissner[i,j], A. Micherdzińska[a], A. Nogga[i], P.U. Sauer[k]
R. Skibiński[b], R. Sworst[b], H. Witała[b] J. Zejma[b], W. Zipper[a]

[a]Institute of Physics, University of Silesia, 40-007 Katowice, Poland
[b]Institute of Physics, Jagellonian University, 30-059 Cracow, Poland
[c]Universidade de Lisboa, CFN, 1649-003 Lisboa, Portugal
[d]Jefferson Laboratory, Theory Division, Newport News, VA 23606 USA
[e]Ruhr Universität Bochum, ITP II, 44780 Bochum, Germany
[f]Kernfysisch Versneller Instituut, 9747 AA Groningen, The Netherlands
[g]Department of Physics, KIT, 804-8550 Kitakyushu, Japan
[h]Institute of Nuclear Physics PAN, 31-342 Cracow, Poland
[i]Universität Bonn, ISKP (Theorie), 53115 Bonn, Germany
[j]Forschungszentrum Jülich, IKP (Theorie), 52425 Jülich, Germany
[k]Universität Hannover, ITP, 30167 Hannover, Germany

(Received November 15, 2005)

A measurement of the analyzing powers for the ${}^1H(\vec{d},pp)n$ breakup reaction at 130 MeV polarized deuteron beam energy was carried out at KVI Groningen. The experimental setup covered a large fraction of the phase space. Obtained tensor analyzing powers T_{22} for selected kinematical configurations have been compared to theoretical predictions based on various approaches: the rigorous Faddeev calculations using the realistic nucleon–nucleon potentials with and without three nucleon force (3NF) models, predictions of the chiral perturbation theory, and coupled channel calculations with the explicit Δ degrees of freedom. In the presented configurations the results of all predictions are very close to one another and there are no significant 3NF influences. Not all of the data can be satisfactory reproduced by the theoretical calculations.

PACS numbers: 21.31.–x, 21.45.+v, 25.10.+s

* Presented at the XXIX Mazurian Lakes Conference on Physics August 30–September 6, 2005, Piaski, Poland.

** Supported by the Polish State Committee for Scientific Research (KBN), grant No. 1P03B02627.

1. Introduction

Developments within the meson exchange theory resulted in constructing of modern nucleon–nucleon (NN) potential models, like Argonne AV18 [1], CD-Bonn [2] and Nijmegen I and II [3]. Calculations with the use of these potentials, when applied to the three-nucleon ($3N$) system, are also supplemented with three-nucleon force (3NF) models. At present, the most commonly used models of such additional dynamics are the upgraded Tucson-Melbourne (TM99) [4] and the Urbana IX [5] forces. It is worth mentioning that there exist different methods of including non-nucleonic degrees of freedom in describing the $3N$ system. An example is the explicit Δ-isobar treatment in the coupled-channel formalism as the method of generating an effective 3NF [6], also quite successful in reproducing the data.

In parallel to the meson exchange theory of semi-phenomenological NN and $3N$ potentials an alternative way of constructing the interaction models for the few nucleon system is being pursued within the effective field theory approach. Developed and applied to describe interactions between pions and matter fields (nucleons, Δ's, heavy mesons) as well as of pions themselves in a systematic and, to a large extent, model-independent manner, this approach is called chiral perturbation theory (ChPT). Recent developments in ChPT lead to NN potentials where the multi-pion exchanges are treated unambiguously according to chiral symmetry. In this way the inconsistencies in constructing the NN and $3N$ potential of the meson exchange based models have been mostly removed and the theory of nuclear forces is set up on a more solid and formal basis. First calculations within the ChPT framework at the NNLO order are quite successful in describing the data for the $3N$ system [7].

The $^1\mathrm{H}(\vec{d}, pp)n$ breakup process, with its three particles in the final state, is an extremely reach field to study non-trivial aspects of the interaction dynamics in the simplest many-nucleon system. Especially, the polarization observables are expected to provide many hints on the details of the structure of the 3NF models. The paper presents the first results of the tensor analyzing powers of the deuteron breakup reaction, which signal a forthcoming large data set of polarization observables, covering a large fraction of the phase space.

2. Measurement and detection system

The experiment was performed at KVI Groningen, with the use of vector and tensor polarized deuteron beam of 130 MeV. The beam was extracted from the ion source, accelerated in the superconducting cyclotron AGOR and guided to the experimental setup, where it was focused to a spot of one millimeter diameter on a liquid hydrogen (LH_2) target. The target was located approximately in the center of the vacuum scattering chamber while

the whole detection system was mounted outside the chamber, in the air. The experimental setup, so-called SALAD (Small Angle Large Acceptance Detector), was designed for registering and identifying charged particles — protons and deuterons. It consisted of two layers of a scintillator hodoscope, transmission ΔE detectors of 2 mm thickness and stopping E detectors, 11.2 cm thick, accompanied by a three-plane Multiwire Proportional Chamber (MWPC), allowing to reconstruct polar and azimuthal angles of the charged reaction products. The detection system covered laboratory polar angles θ between 10° and 35° and the full range of the azimuthal angle ϕ, from 0° to 360° [8].

3. Determination of the beam polarization

The main goal of the reported here work was to obtain the experimental values of the tensor analyzing powers T_{22} for the breakup reaction.

First, the values of the vector and tensor polarizations of the deuteron beam were determined with the help of the elastic scattering events. These data were collected for two polarization states with pure tensor beam polarizations (P_z=0, nominal values of P_{zz} equal to -2 and $+1$, respectively) and for an unpolarized beam ($P_z = P_{zz} = 0$). The actual values of P_{zz} for the two polarized beam states have been found for a few selected kinematical conditions (several angles θ_p). For each θ_p events were sorted with respect to the proton azimuthal angle ϕ with the binning of 10°, and the ratios

$$f_{\mathrm{P}}^{\theta_p}(\phi) = \frac{N_{\mathrm{P}}^{\theta_p}(\phi) - N_0^{\theta_p}(\phi)}{N_0^{\theta_p}(\phi)}\,, \tag{1}$$

were constructed. $N_{\mathrm{P}}^{\theta_p}(\phi)$ and $N_0^{\theta_p}(\phi)$ denote the numbers of the elastic events registered with the polarized and unpolarized beam, respectively, connected by the relation:

$$N_{\mathrm{P}}^{\theta_p}(\phi) = N_0^{\theta_p}(\phi)[1 + g(\phi) + h(\phi)]\,, \tag{2}$$

with

$$\begin{aligned} g(\phi) &= +P_z i T_{11}(\theta_p)\sqrt{3}\cos\phi\,, \\ h(\phi) &= P_{zz}\left(-T_{22}(\theta_p)\frac{\sqrt{3}}{2}\cos 2\phi - T_{20}(\theta_p)\frac{\sqrt{2}}{4}\right)\,. \end{aligned}$$

Thus, the shapes of the experimental ratios (1) are described by the function $g(\phi) + h(\phi)$. Such dependencies were fitted to the data — see Fig. 1 (left panel). The vector and tensor analyzing power values at the selected θ_p angles were taken (in the absence of the experimental data) from calculations with the CD-Bonn and TM99 forces.

From the fits the values of the vector P_z and tensor P_{zz} polarizations were obtained. The results for the tensor beam polarization are independent of the analyzed θ_p (see Fig. 1, right panel), what confirms the right shape of the theoretically predicted functions $T_{22}(\theta_p)$ and $T_{20}(\theta_p)$. The resulting mean values in the two used states are $P_{zz} = -1.346 \pm 0.012$ and $P_{zz} = +0.542 \pm 0.011$, respectively. Vector polarization for these states is close to zero ($P_z = -0.060 \pm 0.007$ and $P_z = +0.016 \pm 0.006$).

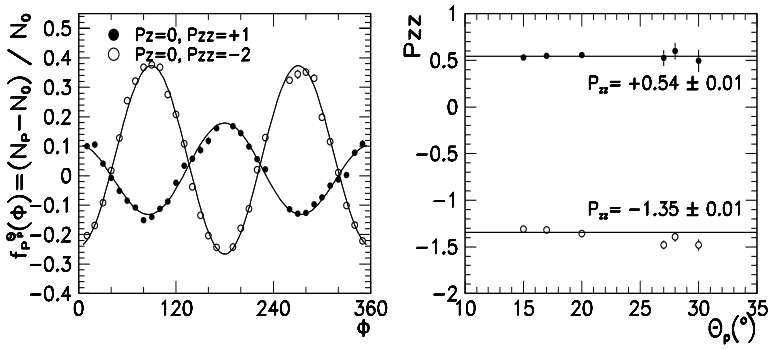


Fig. 1. Left: ratios $f_{\mathrm{P}}^{\theta_p}(\phi)$ for two pure tensor beam polarization states (nominal polarizations shown in the panel), for one chosen proton polar angle $\theta_p = 17^\circ \pm 0.5^\circ$; Right: tensor polarizations P_{zz} obtained for the same two states at several angles θ_p, with the resulting mean values.

4. Breakup analyzing powers T_{22}

The determined above values of the beam polarizations were used to obtain the tensor analyzing powers T_{22} for the breakup reaction.

In the first step, the kinematical spectra E_1 *versus* E_2 were built (as described in [8]) and the events along the kinematical curve were divided into arclength bins with the width of $\Delta S = 16\,\mathrm{MeV}$. The variable S represents the distance, measured along the kinematical curve, from the point of minimal E_2 value. For every bin in S in the selected angular configuration (θ_1, θ_2, ϕ_{12}), the number of the breakup events $N_{\mathrm{P}}^S(\phi)$ was obtained as a function of the azimuthal angle ϕ of the "first" proton. Similar ratios as for the elastic scattering (in Eq. (1) the variable θ_p is replaced by $\xi \equiv (\theta_1, \theta_2, \phi_{12}, S)$, defining a point in the final phase space) were constructed. Again, the ratios can be described by a function $g(\phi) + h(\phi)$ with

$$\begin{aligned} g(\phi) &= +iT_{11}(\xi)P_z\sqrt{3}(\sin\phi + \cos\phi)\,, \\ h(\phi) &= -T_{22}(\xi)P_{zz}\frac{\sqrt{3}}{2}(\sin 2\phi + \cos 2\phi) - T_{20}(\xi)P_{zz}\frac{\sqrt{2}}{4}\,, \end{aligned}$$

which was fitted to the breakup data.

From the fit it is, in principle, possible to obtain the experimental values of the analyzing powers iT_{11}, T_{22} and T_{20} as functions of S in the selected configurations (θ_1, θ_2, ϕ_{12}). However, in the discussed piece of analysis, $P_z \approx 0$ and the sensitivity to iT_{11} is suppressed. In addition, even though T_{20} and T_{22} are always fitted simultaneously, we focus here on T_{22} only, relying rather on the shape of the ϕ distribution than on the absolute value of the ratios. Obtained T_{22} values for the two beam polarization states have been found consistent with each other and the weighted averages of those results were calculated. The examples of T_{22} distributions are presented in Fig. 2.

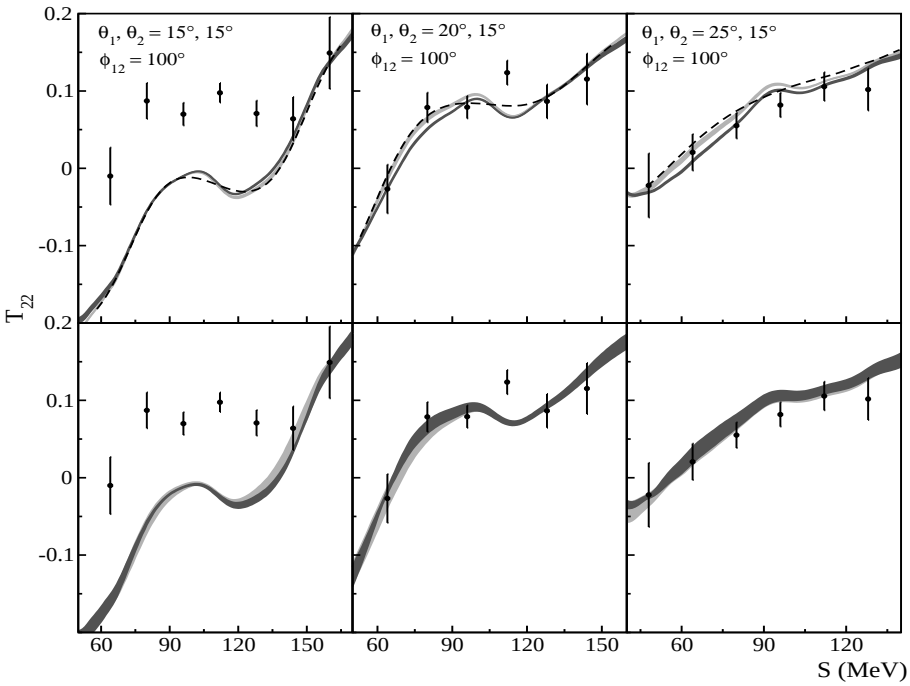


Fig. 2. The breakup analyzing powers T_{22} for 3 kinematical configurations, indicated in the individual panels. The error bars represent the statistical uncertainties. In the *upper part* the results are compared to the predictions based on the realistic NN potentials only (light-grey bands) and with the calculations in which the TM99 3NF has been included (dark-grey bands). The results obtained within the coupled-channel framework with the CD-Bonn+Δ potential are shown as the dashed lines. In the *lower part* the same data are compared to the predictions obtained within the ChPT approach at NNLO: the complete $3N$ calculations (dark-grey bands) and the results for the NN contributions only (light-grey bands).

5. Comparison with theoretical predictions

The experimental results of T_{22} have been compared with various approaches to the theoretical treatment of the $3N$ scattering problem: the predictions based on the realistic NN (CD-Bonn, AV18, Nijm I and Nijm II) potentials only and with the TM99 3NF model included, the results of the coupled-channel calculations with the CD-Bonn+Δ potential, and the predictions obtained within the ChPT framework at NNLO.

Searches for the 3NF effects are particularly well founded in a situation when the data are properly described in the regions of consistency between all the models. Therefore, our studies of T_{22} started in the angular range where the theoretical predictions are very similar in all the approaches (see examples in Fig. 2). The bands of the theoretical predictions are narrow for both, pure NN and NN + 3NF calculations, and the discrepancies between results of these two approaches are small. In the case of the ChPT calculations at NNLO (Fig. 2, lower part), the bands representing the uncertainties of the ChPT predictions have widths comparable with the 3NF effects predicted at this order of calculations.

In two of the three presented configurations the data are very well reproduced by the theoretical predictions. For the configuration $\theta_1 = \theta_2 = 15^\circ$, $\phi_{12} = 100^\circ$ the theories fail in describing the data. In order to trace eventual regularities of the discrepancies a large number of the experimental points will be analyzed, similarly to the cross section case [8]. In the next step of the data evaluation also T_{20} will be extracted, for which large 3NF effects are predicted in some regions. Establishing patterns of (dis)agreements across the phase space for all analyzing powers might help in locating weak points in the present-day understanding of the $3N$ system dynamics.

REFERENCES

[1] R.B. Wiringa, V.G.J. Stoks, R. Schiavilla, *Phys. Rev.* **C51**, 38 (1995).

[2] R. Machleidt, F. Sammarruca, Y. Song, *Phys. Rev.* **C53**, R1483 (1996); R. Machleidt, *Phys. Rev.* **C63**, 024001 (2001).

[3] V.G.J. Stoks *et al., Phys. Rev.* **C49**, 2950 (1994).

[4] S.A. Coon *et al., Nucl. Phys.* **A317**, 242 (1979); S.A. Coon, H.K. Han, *Few-Body Syst.* **30**, 131 (2001).

[5] B.S. Pudliner *et al., Phys. Rev.* **C56**, 1720 (1997).

[6] A. Deltuva, K. Chmielewski, P.U. Sauer, *Phys. Rev.* **C67**, 034001 (2003); A. Deltuva, R. Machleidt, P.U. Sauer, *Phys. Rev.* **C68**, 024005 (2003).

[7] E. Epelbaum *et al., Phys. Rev.* **C66**, 064001 (2002).

[8] St. Kistryn *et al., Phys. Rev.* **C68**, 054004 (2003); St. Kistryn *et al., Phys. Rev.* **C72**, 044006 (2005).